Contribution of blazars to the extragalactic diffuse gamma-ray background and their future spatial resolution

Kevork N. Abazajian, Steve Blanchet, and J. Patrick Harding

Phys. Rev. D **84**, 103007 — Published 18 November 2011

DOI: 10.1103/PhysRevD.84.103007

UMD-PP-10-022

The Contribution of Blazars to the Extragalactic Diffuse Gamma-ray Background and Their Future Spatial Resolution

Kevork N. Abazajian[1,2],* Steve Blanchet[2,3],† and J. Patrick Harding[2‡]
[1] *Department of Physics and Astronomy, University of California, Irvine, Irvine, California 92697 USA*
[2] *Maryland Center for Fundamental Physics & Joint Space-Science Institute, Department of Physics, University of Maryland, College Park, Maryland 20742 USA and*
[3] *Instituto de Física Teórica, IFT-UAM/CSIC Nicolas Cabrera 15, UAM Cantoblanco, 28049 Madrid, Spain*

We examine the constraints on the luminosity-dependent density evolution model for the evolution of blazars given the observed spectrum of the diffuse gamma-ray background (DGRB), blazar source count distribution, and the blazar spectral energy distribution sequence model, which relates the observed the blazar spectrum to its luminosity. We show that the DGRB observed by the Large Area Telescope (LAT) aboard the *Fermi Gamma Ray Space Telescope* can be produced entirely by gamma-ray emission from blazars and non-blazar active galactic nuclei, and that our blazar evolution model is consistent with and constrained by the spectrum of the DGRB and flux source count distribution function of blazars observed by Fermi-LAT. Our results are consistent with previous work that used EGRET spectral data to forecast the Fermi-LAT DGRB. The model includes only three free parameters, and forecasts that $\gtrsim 95\%$ of the flux from blazars will be resolved into point sources by Fermi-LAT with 5 years of observation, with a corresponding reduction of the flux in the DGRB by a factor of $\sim$2 to 3 (95% CL), which has implications for the Fermi-LAT's sensitivity to dark matter annihilation photons.

PACS numbers: 98.62.-g,98.62.Js,98.62.Ve,95.35.+d

I. INTRODUCTION

The source of the extragalactic isotropic diffuse gamma-ray background (DGRB) has been an unsolved question in astrophysics for some time. In this paper, we show how the DGRB spectrum can be produced by a combination of blazar and non-blazar active galactic nuclei (AGN) gamma-ray sources. We also show that the blazar flux source count distribution function (dN/dF) is consistent with the full DGRB originating from these sources. Furthermore, we show how less-detailed models of the blazar contribution failed to be consistent with the DGRB. We explore how the implications for dark matter detection or constraints from the DGRB will evolve as the blazar sources of the DGRB are resolved.

The DGRB was first discovered by the SAS 2 experiment in 1975, for gamma-ray emission in the range of 35 to 300 MeV [1]. This background was seen at energies up to 20 GeV by the EGRET collaboration, and it was confirmed at these energies in the first-year data from the Large Array Telescope (LAT) aboard the *Fermi Gamma-Ray Space Telescope* [2–4]. The assumed extragalactic source of the DGRB is determined by measuring the complete diffuse (unresolved) flux and then subtracting off a model to account for the background coming from our Galaxy. This yields a measure of the flux coming from unresolved diffuse sources, presuming there is no minimal isotropic component from the Galaxy, e.g. dark matter annihilation or decay. The DGRB has been used to constrain dark matter annihilation in Galactic and extragalactic sources [5–7].

The most recent measurement of the DGRB was performed by the Fermi-LAT. In the Fermi-LAT collaboration analysis, the gamma-ray intensity was measured in the range of 100 MeV to 100 GeV above 10° in Galactic latitude ($|b| > 10°$). The total flux is modeled by stacking the spectra of known sources with the cosmic-ray background, the Galactic diffuse background, and the DGRB. This analysis gives an DGRB intensity that is roughly 25 percent of the total observed flux. The DGRB seen by the Fermi-LAT is consistent with a power-law in energy with index 2.41. This value for the DGRB is notably softer at high energies than was previously seen in the EGRET collaboration, which is partly due to an updated model of the diffuse Galactic emission in Ref. [3] (hereafter FS10).

A detailed spectral energy distribution (SED) sequence model of blazars can reproduce the DGRB [8, 9]. We explore this model in this work. Many models have been proposed to explain the DGRB. It has been shown that emission from AGN can account for the diffuse background from 10 keV to 100 MeV, but above that energy, this model cannot account for the large gamma-ray flux [10]. Radiation from star-forming galaxies could account for much of the DGRB up to 10 GeV, but this also cannot explain the high intensities observed at higher energies [11]. Emission from millisecond pulsars has been proposed as a source as well [12]. However, millisecond

* kevork@uci.edu
† steve.blanchet@uam.es
‡ hard0923@umd.edu

pulsars as a dominant source of the DGRB may be inconsistent with the lack of anisotropy in the DGRB [13].

Dark matter annihilation, both as a component of the extragalactic diffuse emission and as an unaccounted foreground from the Milky Way can contribute to the DGRB, but the fluxes from dark matter are expected to be lower than the DGRB flux and have a different spectral shape [5, 6]. However, measurements of the DGRB are one of the strongest ways to constrain dark matter annihilation [7]. If dark matter is a significant contributor, it may be disentangled from astrophysical sources due to its angular correlation on the sky [14]. Pioneering work proposed that blazars could account for *all* of the DGRB seen by the EGRET collaboration [15]. The blazar class of AGN has been studied in depth as the origin of the DGRB at high energies [15–26].

In Ref. [8] it was shown that the DGRB can be composed of blazars and non-blazar AGN in the luminosity-dependent density evolution (LDDE) spectral energy distribution (SED) blazar model. This model contains only three free parameters describing the gamma-ray luminosity function (GLF) of blazars. We show that this model is consistent with producing the full DGRB spectrum as well as the blazar source count distribution, dN/dF, of blazars as measured by Fermi-LAT. In addition, we constrain this model by these measurements and find parameters for which the model successfully reproduces these measurements. Note that both the source count distribution dN/dF and DGRB spectrum are predicted by the model, and not an input to the model.

Recent work by the Fermi-LAT collaboration found that the DGRB could not be composed entirely by blazars [4] (hereafter FB10). However, that work adopted an over-simplification of the blazar SED to be a single power-law (PL), independent of blazar luminosity, which is inconsistent with the observed spectral luminosity dependence seen in the SED sequence [27]. In contrast, in a separate paper, the Fermi-LAT collaboration emphasizes the need for including departures from pure-PL behavior in blazar spectra when calculating the contribution of unresolved low-luminosity blazars to the DGRB [28]. Incorporating the SED departure and its dependence on blazar luminosity evolution when modeling the DGRB is exactly the intent of the work presented here.

Furthermore, the blazar model in FB10 lacks a physical evolution model for blazars. Instead of the source count distribution resulting from the cosmological evolution of blazars, the source count distribution is an input to the model, as a broken power-law with four free parameters. Note that even though the model in FB10 is simplistic, it contains *more* free parameters than the LDDE plus SED-sequence model explored here. In our approach there are three parameters in the adopted blazar model which describe the relation between the GLF and X-ray luminosity function (XLF). Because the FB10 model employs a pure-PL luminosity-independent SED with a broken-PL source count distribution, the conclusions of that work do not apply to the model examined here. Other parameters in our work (*e.g.*, the SED sequence and the low-energy non-blazar AGN model) are constrained by other observations and remain fixed in our blazar model analysis. Namely, the observational constraints on the SED sequence come from spectral population models of blazars as in [27], and the non-blazar AGN spectrum is constrained by the hard X-ray luminosity function derived from *HEAO1*, *ASCA*, and *Chandra* X-ray AGN surveys [10, 29].

A recent paper by Malyshev & Hogg [30] using the one-point PDF of the DGRB also concludes that blazars cannot constitute the total DGRB flux as measured by Fermi-LAT, when modeled as a pure-PL SED with a fixed dN/dF. However, this conclusion also only applies to the model which they consider, which adopt blazars as having pure-PL luminosity-independent SEDs, and not to the LDDE SED-sequence model examined here.

Because observed blazars make up about 15 percent of the total gamma-ray flux, unresolved blazars are a likely candidate to make up the DGRB [2, 4]. Blazars were the most numerous point-source objects observed by the EGRET collaboration [31]. Additionally, observed blazar spectra tend to follow a similar power-law in energy as the DGRB. However, it is known that blazars have a luminosity-dependence to their spectral shape, which is incorporated in the SED sequence model [27], but ignored in the analysis of FB10.

Blazars are the combination of two classes of AGNs: flat-spectrum radio quasars (FSRQs) and BL Lacertae objects (BL Lacs). FSRQs are AGNs that have spectral index $\alpha_r < 0.5$ in the radio band and have radio emission lines with equivalent width greater than 5 Å. BL Lacs have no strong absorption or emission features, and have equivalent widths less than 5 Å [32]. Broadly speaking, blazars tend to have their bolometric luminosities dominated by the gamma-ray luminosity and have great variability in that luminosity. Therefore, it is believed that blazars represent the small set of AGN that are observed along the jet axis, as opposed to non-blazar AGNs which are observed far from the jet axis and dominate emission by their luminous accretion disk. This jet source is expected to be relativistically beamed, as opposed to the more isotropic flux coming from the AGN's accretion disk [33, 34].

Different models of blazar emission have been proposed in the literature [15–26]. One is the pure luminosity evolution (PLE) model of the distribution of blazars [19, 20, 24, 26]. In this model, only the blazar luminosity is evolved in redshift. An alternative model, LDDE, relates the gamma-ray luminosity of blazars to the redshift-dependent distribution of X-ray emission from non-blazar AGN [23]. This technique more realistically fits the blazar evolution to the AGN distribution, rather than assuming that all blazars have identical evolution regardless of luminosity. In many models for blazar spectra, a simple power-law or distribution of power laws is used as the intrinsic blazar spectrum, but more detailed frequency-dependent models have been used as well [22].

Here, we employ the LDDE model for blazar distributions. For the intrinsic spectrum of blazars, we use a frequency-dependent SED based on the multi-wavelength study of Refs. [27]. We use these models to derive the differential blazar spectrum in redshift, luminosity, and energy. By integrating over these variables, we can determine the number of detectable blazars for given detector sensitivities, and we can calculate the expected gamma-ray flux from unobserved blazars to determine how significantly they contribute to the DGRB. Additionally, we add a fixed non-blazar AGN component to our predicted blazar flux, which should make the net flux from our model fit the diffuse background over the energy range from 10 keV to 100 GeV.

Below, we begin by describing the DGRB seen by the Fermi-LAT as well as its data on blazars. We will then describe our model in detail, specifying the evolution model and SED used in our calculations and how we fit these to the known data. We use this model to predict the ability of the Fermi-LAT to detect blazars and how this will affect the DGRB. Throughout the paper, we take a flat universe with the cosmological parameters $\Omega_m = 0.272$, $\Omega_\Lambda = 0.728$, and $H_0 = 70.2$ km s^{-1} Mpc^{-1} [35]. *Note,* the use of h in the text refers to Planck's constant, and not the Hubble parameter.

II. FIRST-YEAR FINDINGS BY THE FERMI-LAT COLLABORATION

A. DGRB Measurements

From its first year of data, the Fermi-LAT has measured a spectrum for the DGRB (FS10). To get this spectrum, the total gamma-ray intensity had known sources subtracted from it, as well as the background from cosmic rays, and the expected galactic diffuse emission. At this time, resolved extragalactic sources account for about 15 percent of the total gamma-ray flux in the sky. To calculate the gamma-ray emission from Galactic cosmic rays, the local cosmic-ray spectra are extrapolated to give source populations, which are then propagated through appropriate target distributions using the GALPROP particle propagation package [36, 37]. This diffuse Galactic emission is the largest component of the DGRB, comprising roughly half of the total observed intensity. A small component to the DGRB is a background due to cosmic ray interaction with the Fermi-LAT itself. This background has been studied in detail in FS10 and is very well characterized. This background accounts for 1 to 10 percent of the total emission, with a greater fraction at low energies and a lesser fraction at high energies. The residual intensity after all of these components have been removed is called the isotropic DGRB. It makes up around 25 percent of the total emission. Because of the model dependence of these subtractions, the uncertainties on the DGRB are dominated by systematics (FS10). The DGRB may come from unresolved extragalactic sources or unaccounted Galactic sources, such as millisecond pulsars, or, potentially, from Galactic dark matter annihilation or decay.

B. Point Source Sensitivity

The Fermi-LAT detector has a spectrally-dependent point source sensitivity due to the higher spatial resolution of the instrument to higher-energy photons. The flux limit to point sources is shown in Fig. 1, along with the sample of blazar fluxes and spectral indices from FB10. In FS10, the DGRB spectrum is compared to that measured by EGRET, which had a point source sensitivity of 1×10^{-7} ph cm^{-2}s^{-1}, despite the fact that the point source sensitivity of the two instruments, and therefore the measured DGRB flux between the two instruments' measurements, are quantitatively different.[1] We derive the flux limit from the sample of blazars used in FB10, using the lowest-flux end of the blazar sample, which satisfied the test-statistic $TS = 25$. In FB10, the source count distribution and DGRB spectrum was fit with only blazars resolved at $TS = 50$, therefore, the point source limit is augmented by a factor of two, as shown by the solid in Fig. 1, with the point source sensitivity always below or equal to Fermi-LAT's believed completeness for all spectra sources at 7×10^{-8} ph cm^{-2}s^{-1}.

Importantly, it should be made clear that a fixed point source sensitivity cannot be exactly specified for the DGRB spectrum derived in FS10. In that work, all sources above a $TS = 200$ are allowed to vary in the amplitude of their flux during the fitting of the extragalactic isotropic DGRB. Therefore, the exact flux-limit of the DGRB spectrum, and therefore the nature of the spectrum itself, as presented in FS10, is ill-defined. We therefore adopt the best-estimate method of modeling the DGRB spectrum as done by the Fermi-LAT collaboration itself in FB10, with a $TS = 50$ spectrally-dependent flux limit. We define the power-law photon index Γ for the non-power-law SED sequence model of a blazar by fitting a power-law to the Poisson-limited spectrum within the observed energy range of Fermi-LAT.

As the point-source sensitivity of Fermi-LAT improves with integration time, the resolution of the extragalactic DGRB into point sources will not proceed proportionally to the sensitivity, but rather in a combination of the sensitivity with where the population of extragalactic emitters lies with respect to that sensitivity/spectral-index plane. In particular, for the LDDE plus SED-sequence blazar model here, there are more hard-spectrum sources

[1] Due to this direct comparison in FS10, in the v1 preprint of this work, a point source sensitivity cutoff of the measured DGRB spectrum of FS10 was adopted to be 1×10^{-7} ph cm^{-2}s^{-1}, instead of the spectrally-dependent sensitivity here. This does not change our conclusions, but does modify our best fit model parameters and our 5-year forecast DGRB spectra.

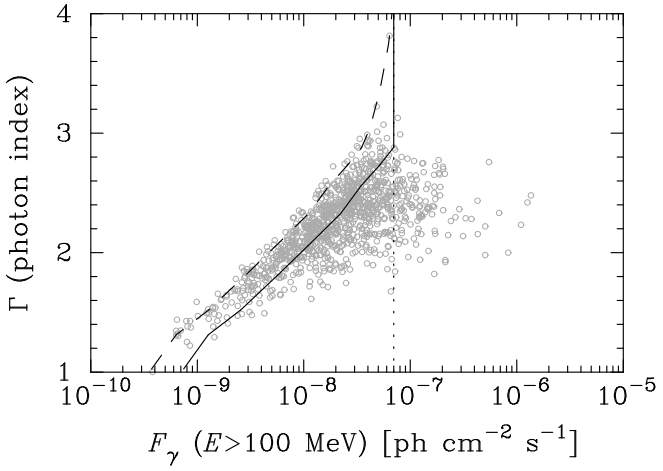

FIG. 1. Shown is a sample of the blazar gamma-ray fluxes above 100 MeV (F_{100}) versus their power-law fit spectral-index Γ from FB10. The blazars (points) are shown above point-source detection test-statistic $TS = 25$ (with the corresponding point-source limit shown as the dashed line), while those below $TS = 50$ are modeled, in our work and in FB10, to contribute to the DGRB as measured by FS10 (with point-source limit shown by the solid line). Note the total luminosity vs. spectrum dependence of the blazar population evident in this plot. The first year Fermi-LAT point source sensitivity is complete above the dashed line at 7×10^{-8} ph cm^{-2}s^{-1} (FB10).

with lower gamma-ray flux. This trend already can be seen in the plotted blazar points in Fig. 1.

C. Blazar Measurements

Through one year of running, the Fermi-LAT has detected a total of 296 FSRQs, 300 BL Lacs, and 72 blazars of unknown type. The observed FSRQs have an average spectrum with photon index 2.48 and BL Lacs have average photon index of 2.07 [38]. This power law index is similar to the DGRB power law index of 2.41, which suggests that unresolved blazars could be the primary source of the DGRB. Additionally, the stacked spectra of known blazars detected by the Fermi-LAT is responsible for 15 percent of their total observed gamma-ray emission observed by the Fermi-LAT. The number of blazars observed above a given flux tends to follow a broken power-law, with a break at $F(> 100\ \mathrm{MeV}) = 6 \times 10^{-8}$ photons cm^{-2} s^{-1}. This break seems to be independent of detector sensitivity, because the sensitivity dies off much more quickly as a function of flux than the blazar number count (FB10).

In the Fermi-LAT measurements, FSRQs and BL Lacs have similar variability properties, so the assumption that they are of one class appears valid. For BL Lacs, the LAT has detected significantly more hard-spectrum sources than soft-spectrum sources, which is consistent with the known selection bias in the measurement. FSRQs peak at a redshift of unity, indicating that the sample is approaching completeness. In contrast, BL Lacs peak at low redshift, indicating that the sample is not yet complete. FSRQs tend to be more luminous than BL Lacs: FSRQs have radio luminosities that peak at $L_{\rm rad} \approx 10^{44.5}$ erg/s whereas BL Lacs have lower radio luminosities peaking at $L_{\rm rad} \approx 10^{42}$ erg/s [38]. This would indicate that there is a fairly large contribution of low-luminosity, soft-spectrum BL Lacs that has yet to be resolved.

The differences in spectra between FSRQs and BL Lacs is significant. The average gamma-ray photon index is roughly 0.5 larger for FSRQs than for BL Lacs. Even among BL Lacs themselves, high-synchrotron-peak BL Lacs (HSP-BL Lacs) have a photon index of 2.28 while low-synchrotron-peak BL Lacs (LSP-BL Lacs) have a photon index of 1.96. FSRQs give off their peak synchrotron radiation at around 10^{13} Hz whereas for BL Lacs, the distribution is much broader, stretching from 10^{12} Hz to 10^{17} Hz [38]. FSRQs have their inverse Compton (IC) peaks at energies less than 100 MeV, so power-law fits work fairly well to match their LAT-measured spectra. For BL Lacs, the peak IC emission tends to lie in the LAT's energy range, with LSP-BL Lacs peaking closer to 100 MeV and HSP-BL Lacs peaking closer to 100 GeV. Because of these peaks, these spectra do not match a power-law, though a broken power-law can approximately fit them [28].

To truly model the blazar SED, a multi-wavelength analysis is needed [27]. The Fermi-LAT collaboration did a multi-wavelength study of the spectra of blazars, combining the results of several radio, X-ray, optical, and gamma-ray blazar studies [39]. This study found strong correlation between the X-ray and gamma-ray spectral slopes, indicating that blazar spectra fit a two-peaked, synchrotron plus IC scenario well. They found that BL Lacs have larger synchrotron peaks than FSRQs, which explains why BL Lacs have harder gamma-ray indices. This study plotted the SED for several blazars, all of which have a strong double-peaked shape when luminosity is plotted versus frequency on a log-log plot. This is consistent with previous analyses of the blazar SED [27].

III. DETERMINATION OF BLAZAR FLUX AND SPECTRUM

A. Spectral Energy Distribution

The model of blazar emission we use consists of two parts: a gamma-ray luminosity function (GLF) to give the density of blazars per unit luminosity and an SED to determine the luminosity of blazars as a function of energy. These are denoted by $\rho_\gamma(L_\gamma, z)$ and $\nu L_\nu(x; P)$, where z is redshift of the blazar, L_γ is the gamma-ray luminosity (defined as νL_ν at $h\nu = 100$ MeV), $x \equiv \log(\nu/\mathrm{Hz})$ for blazar rest-frame frequency ν, and P

is the bolometric luminosity. Because our SED separates blazars according to radio luminosity, the bolometric luminosity is used to determine which SED curve matches a given blazar. For a given SED curve, the bolometric luminosity can be calculated as $\int L_\nu d\nu$. This can then be used to find the gamma-ray luminosity.

Refs. [27] analyzed the relationship between frequency and luminosity for blazars. To get these relationships, blazars were binned by radio luminosity. This analysis showed that blazar gamma-ray index is correlated with blazar luminosity. This correlation is consistent with the experimental results that FSRQs have high luminosities and large gamma-ray spectral indices while BL Lacs have lower luminosities and smaller spectral indices [28, 39, 40]. A proper calculation using blazar spectra should account for this relationship between index and luminosity, and not simply use a power-law in energy for the blazar spectrum. Note that this was not done in Ref. [4], which claimed that blazars cannot constitute the full DGRB.

For the frequency dependence of the blazar luminosity, we use the SED sequence of Inoue & Totani [8]. In this model, blazars SEDs are fit over frequencies from radio to gamma-ray, as in Refs. [27]. Each SED is comprised of two components, a synchrotron component at lower energies and an IC component at higher energies. These are each parameterized by a parabolic peak with a lower-energy linear tail. The details of the model are determined by fitting to the data in Refs. [27], which give νL_ν as a function of rest-frame frequency ν for five luminosity bins. This provides the gamma-ray luminosity (νL_ν at $h\nu = 100$ MeV), the specific luminosity $L_\nu(\nu)$, and the bolometric luminosity $\int L_\nu d\nu$ for a blazar with known radio band luminosity (νL_ν at 5 GHz). The full model can be found in Appendix A.

As a check on the versatility of the SED model, we explicitly compared the model to several blazar spectra measured by the Fermi-LAT collaboration [28, 39]. The model fit the data in the Fermi-LAT energy range well. It also matched the data qualitatively: the model spectra had increasing, decreasing, or flat spectral shapes in agreement with the Fermi-LAT-measured spectra. Such agreement indicates that this SED fit approximates the full blazar SED well.

B. Gamma-Ray Luminosity Function

For the distribution of gamma-ray blazars, we follow the hard X-ray AGN distributions parameterized by Ueda et al [29]. Similar work was done for soft X-rays by Hasinger et al [41]. However, the hard X-ray parameterization gives a more conservative prediction of blazar detection by Fermi-LAT, so we use that here. For rest-frame (emission frame) energy of $\epsilon_{\rm gam,res} = 100$ MeV, the gamma-ray luminosity is given by $L_\gamma \equiv (\epsilon_{\rm gam,res}/h) L_\nu(\epsilon_{\rm gam,res}/h, P)$.

Ref. [8] argues that the gamma-ray luminosity can be related to the X-ray AGN disk luminosity L_X through the bolometric luminosity by $P = 10^q L_X$, where q is a scaling parameter. This is because the bolometric luminosity from a blazar jet is proportional to the mass accretion rate $\dot{m}$. For blazars with low accretion rate, the conversion of power into luminosity is inefficient, with $L_X \propto \dot{m}^2$. For blazars with high accretion rate close to the Eddington limit, the conversion is efficient and the disk luminosity goes as $L_X \propto \dot{m}$ [42–44]. Because black hole growth takes place mostly near the Eddington limit, it is reasonable to assume that $P \propto \dot{m} \propto L_X$ [45]. Note, L_X is the X-ray luminosity from the accretion disk of the blazar, not to be confused with the X-ray luminosity of the beam.

The comoving number density per unit L_γ of gamma-ray blazars is

$$\rho_\gamma(L_\gamma, z) = \kappa \frac{dL_X}{dL_\gamma} \rho_X(L_X, z), \tag{3.1}$$

where ρ_X is the comoving number density of AGN per unit L_X, z is the redshift to the source, and κ is the fraction of AGN observed as blazars. The quantity ρ_γ is referred to as the GLF. A parameterization of the X-ray luminosity function ρ_X is found in Appendix B. The GLF has three free parameters: q determines the ratio of bolometric jet luminosity to accretion-disk X-ray luminosity, γ_1 is the faint-end index that determines how the GLF behaves for low luminosities, and the blazar fraction is κ.

These GLF models are based on LDDE of AGNs, as opposed to PLE models. In PLE models, AGN luminosity changes with redshift, but the comoving density of AGN remains constant. This has been a popular method of determining blazar parameters [19, 20, 24, 26]. LDDE models have the peak evolution redshift depend on luminosity, so AGN of different luminosities will have slightly different evolutions [29, 41]. This gives a better fit to the AGN data and should describe blazar evolution more fully than PLE models [23]. The exact relationship between X-ray AGN and gamma-rays blazars is not yet known. We are using the simple ansatz that they are related as shown in Eq. (3.1), as proposed by Inoue and Totani [8]. To the best of our knowledge, this model satisfies all current observations and constraints, and therefore is a viable possibility.

C. Calculation of Blazar Number and Flux

For a given blazar, the gamma-ray flux observed on Earth is

$$F_\gamma(z, P) = \frac{1+z}{4\pi d_L(z)^2} \int_{E_{\rm min,obs}(1+z)/h}^{\infty} d\nu \frac{L_\nu(\nu, P)}{h\nu}, \tag{3.2}$$

where d_L is the luminosity distance, P is the bolometric luminosity, and $E_{\rm min,obs} = 100$ MeV is the minimum observable photon energy on earth by the Fermi-LAT.

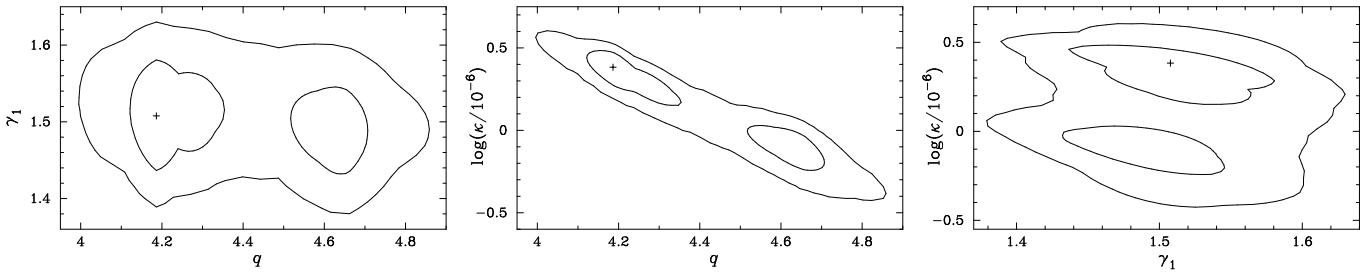

FIG. 2. Shown are contours with 68% and 95% confidence level (CL) regions for the parameters of the luminosity scale q and GLF faint-end index γ_1, q vs. κ, and κ vs. γ_1. The best-fit value is labeled by the cross.

With the GLF and SED, the number count of blazars detected above a sensitivity F_γ is

$$N(>F_\gamma) = 4\pi \int_0^{z_{\rm max}} dz \frac{dV}{dz} \int_{L_\gamma^{\rm lim}(z,F_\gamma)}^{\infty} dL_\gamma \rho_\gamma(L_\gamma, z), \tag{3.3}$$

where $L_\gamma^{\rm lim}$ is the luminosity below which a blazar at redshift z is no longer detectable for the sensitivity F_γ. We set the parameter $z_{\rm max} = 5$, but this does not affect the calculation significantly, since the peak distribution is at redshift of order unity.

The diffuse flux coming from unresolved blazars is given by

$$\begin{aligned}\frac{dN}{dE_{\gamma 0} dA dt d\Omega} =& \frac{1}{4\pi} \int_0^{z_{\rm max}} dz \frac{d\chi}{dz} e^{-\tau(z,E_{\gamma 0})} \\ &\times \int_{L_{\gamma,\rm min}}^{L_\gamma^{\rm lim}(F_\gamma,z)} dL_\gamma \frac{\rho_\gamma(L_\gamma, z)}{h} \\ &\times \frac{L_\nu[E_\gamma/h, P(L_\gamma)]}{E_\gamma}. \end{aligned} \tag{3.4}$$

Here, E_γ is the emitted photon energy (and $E_{\gamma 0} = E_\gamma/(1+z)$ is the observed photon energy at Earth), A is area on Earth, t is time on Earth, and Ω is solid angle in the sky. Here $L_\nu/(E_\gamma)$ is the number of photons emitted per rest-frame frequency per rest-frame time per blazar (h is Planck's constant). The quantity $dL_\gamma \rho_\gamma$ is the number of blazars per comoving volume. The integral $d\chi$ is the line-of-sight integral over the comoving distance. Because for $\gamma_1 > 1$ the integral diverges at zero luminosity, $L_{\gamma,\rm min}$ is a lower bound on the luminosity integral. We choose $L_{\gamma,\rm min} = 10^{42}$ erg s^{-1} which is an order of magnitude lower than any Fermi-LAT observed blazar [28, 39]. That is, we impose a step-function cutoff of blazar GLF. The final result is not strongly dependent on the value of this cutoff, with a two-order of magnitude difference in $L_{\gamma,\rm min}$ modifying our best fit parameters by $\sim$25%.

The $\exp(-\tau)$ factor in the diffuse flux calculation accounts for absorption of the photons on intergalactic background radiation before reaching Earth. We use the absorption factor from Gilmore et al. [46]. This absorption factor was determined through the use of galaxy formation models to find the contribution of starlight to the absorption, as well as a contribution from quasars which is calculated based on empirical data. This model predicts lower values of the opacity τ than previous estimates, which leads to less expected absorption. This is consistent with the Fermi-LAT observing several high-energy photons coming from fairly high redshifts, and this opacity is consistent with the findings of Ref. [47].

D. DGRB Spectrum Calculation

In addition to the blazar contribution to the DGRB flux, we also include a non-blazar AGN component to our DGRB spectrum calculation. Ref. [10] has shown that non-blazar AGN can account for the background radiation down to keV energies. The combination of blazars with non-blazar AGN gives a unified model that can explain the diffuse high-energy X-ray to gamma-ray background over eight orders of magnitude in energy.

The AGN model we use is the model of Ref. [10]. This model assumes the usual thermal electrons from AGN coronae, but it includes a high-energy non-thermal component as well. These electrons Comptonize, which produces the known X-ray spectra of AGN. This high-energy component is analogous to the emission from solar coronae in solar flares. Such electrons are assumed to have a power-law injection spectrum $dN/dE \propto E^{-\Gamma}$. By adding this non-thermal electron source to the usual thermal one, it is found that the model matches the diffuse background spectrum well from energies from keV to tens of MeV.

Specifically, we choose the $\Gamma = 3.5$ non-blazar AGN model of Ref. [10], which we increase in amplitude by a factor of two in order to match 50% of the amplitude of the lowest energy point in the Fermi-LAT DGRB spectrum, with a broken power law matching the measurements of the diffuse background by the COMPTEL collaboration [48]. The power-law slope of the non-blazar AGN spectrum is fixed by modeling of the hard X-ray luminosity function from X-ray AGN surveys [10, 49], and the amplitude is fixed to match the lowest point in the Fermi-LAT DGRB spectrum. This amplitude is fixed throughout our fitting. In order to reflect the uncertainty of the amplitude of the flux in the lowest energy

bin, we allow for it to have an amplitude uncertainty of 10%, which we vary and show in Fig. 3. Another low-energy emission source, such as millisecond pulsars or star-forming galaxies, may be responsible for the lowest-energy portion of the DGRB, but our analysis is not strongly dependent on the spectral shape taken by the low-energy emission source. For example, the gamma-ray spectrum from star-forming galaxies in Ref. [11] has a similar shape and potential amplitude as the non-blazar AGN component.

In our blazar model, there are three free parameters, in addition to those fixed in the non-blazar AGN model, as described in §III B: q, γ_1, and κ. All other parameters in the blazar model are fixed to valued based on data from other observations such as the SED sequence. It is the purpose of this paper to determine how well unresolved blazars can reproduce the DGRB. Therefore, we simultaneously fit to the blazar source count distribution dN/dF from Ref. [4] and the DGRB spectrum from FS10. This simultaneous fit allows some freedom in the blazar spectrum while still conforming to known blazar number distributions. We can use the results of such a fit to constrain models of the DGRB from unresolved blazars and predict a consistent model of the 5-year Fermi-LAT measurements of the DGRB.

Fitting the model to the blazar dN/dF and the DGRB spectrum, we found that a simultaneous fit was quite reasonable. We set the lowest blazar luminosity as $L_{\gamma,\rm min} = 10^{42}$ erg s^{-1}, as discussed above. The best-fit values we get are $q = 4.19^{+0.57}_{-0.13}$, $\gamma_1 = 1.51^{+0.10}_{-0.09}$, and $\log(\kappa/10^{-6}) = 0.38^{+0.15}_{-0.70}$ (95% CL). The best-fit 68% and 95% confidence level (CL) regions for q and γ_1 are shown in Fig. 2. These are consistent with previous work [8], though more constrained because we are also fitting the source count distribution function dN/dF. The model reproduces the DGRB and blazar dN/dF, with a reduced $\chi^2/{\rm DOF} = 0.63$. The value of q indicates that the bolometric luminosity of a blazar jet is roughly 15 thousand times more luminous than the X-ray from the accretion disk. Here, $\gamma_1 > 1.0$ so low-luminosity blazars have significant contributions to the total blazar flux. Therefore, a ten or more order-of-magnitude lower value of $L_{\gamma,\rm min}$ would modify the calculation considerably, though no blazars have been detected below our $L_{\gamma,\rm min}$ threshold, and therefore it seems unlikely that there is a large population of very-low luminosity blazars. The fraction $\kappa \simeq 2.4 \times 10^{-6}$ implies that there is roughly one blazar for every 420 thousand non-blazar AGN. Our fit to the DGRB spectrum is shown in Fig. 3 and the fit to dN/dF is in Fig. 4.

Our value for the AGN XLF and blazar GLF ratio κ, 3.4×10^{-6} to 5×10^{-7} (at 95% CL), is similar to and slightly larger than the central value derived by Inoue & Totani [8], 1.7×10^{-6}. This implies that only a small fraction of X-ray loud AGN are visible as gamma-ray blazars. The intrinsic jet opening angle of a blazar has been found to be ~ 1 deg (subtending an area of $\sim 2 \times 10^{-4}$ steradian) [51]. Following from this is that only $\sim 2 \times 10^{-5}$ of the AGN jets are potentially visible as blazars. Our model then requires that only $\lesssim 20\%$ of AGN jets are gamma-ray blazars. This is not inconsistent with jet models [52], though if this fraction drops considerably (i.e., κ is required to be much smaller), then it would call into question the blazar model analyzed here.

Note that using the dN/dF estimated from a power-law blazar spectrum model is not perfect, due to the fact that the detection efficiency estimate depends on the spectral model [4]. However, Ref. [4] tested the dN/dF dependence on the sensitivity estimate with a non-power-law fit to the blazar spectra and found it did not significantly change the measurement of dN/dF. We also verified this sensitivity dependence with a test fitting by increasing the errors on the measured dN/dF at low flux, and we found that our model did not prefer a different amplitude or shape to the source counts at the low flux where the efficiency for blazar detection is low.

Refs. [8, 9] used a combined GLF plus SED model to predict the Fermi-LAT's ability to observe blazars and their spectra, using the results of the EGRET collaboration. The paper fit its GLF parameters using the redshift and gamma-ray luminosity distributions of EGRET blazars. This led to a prediction that 600 to 1200 blazars should be resolved in 5 years of Fermi-LAT data, which would yield 98% to 100% of the total blazar flux. However, the cumulative number of blazars predicted by that paper is in disagreement with the observations of the Fermi-LAT [4]. The cumulative number count by Ref. [8] is predicted to have a break at 10^{-7} photons cm^{-2} s^{-1} whereas the break seen by the Fermi-LAT collaboration is at 5×10^{-8} photons cm^{-2} s^{-1}. Also, the surface density of sources predicted in that paper is too small to match the measured value.

Importantly, Refs. [8, 9] fit their model to the EGRET catalog blazar spectra SED, not that from Fermi-LAT. The EGRET telescope had strong cuts which limited high-energy photon observations, which lead to EGRET only observing few BL Lacs [4]. Also, the redshift and luminosity distributions are strongly dependent on detector sensitivity, because BL Lacs have lower luminosity and therefore are observed at lower redshifts. This means that the current data for the overall blazar redshift distribution, in particular, is more strongly biased toward lower redshifts than the complete distribution. Ref. [53] posited that one significant source for the difference between this calculation and the Fermi-LAT results comes from needing to correctly account for Fermi-LAT sensitivities. By fitting to dN/dF, which is not as heavily dependent on detector sensitivity, we can get a more robust prediction that should not change significantly for different sensitivities. Refs. [8, 9] argued that a model of this type should roughly match the DGRB spectrum. In Ref. [8], the model parameters were fit to the EGRET DGRB spectrum, and, as discussed above, the model parameters are roughly consistent with our results. In our analysis here, we use the DGRB spectrum and flux source counts, as measured by the Fermi-LAT, as a constraint

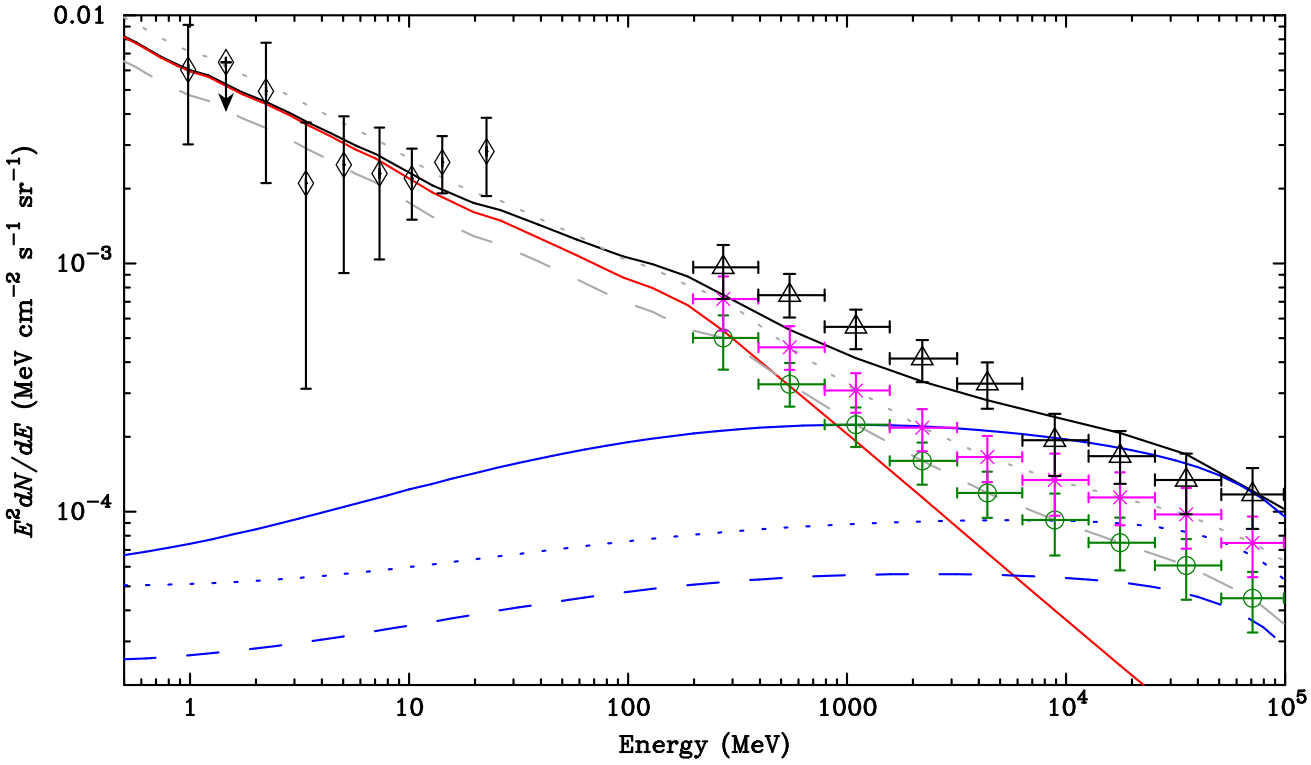

FIG. 3. Shown are the best-fit model for the current DGRB spectrum (solid black line) and our upper/lower 95% CL forecast for the Fermi-LAT 5-year sensitivity (magenta/green points). The solid red line is the AGN flux from Ref. [10]. The blue lines are the blazar contribution to the DGRB for the current (solid), and predictions for the most-optimistic (dashed) and least-optimistic (dotted) 95% CL 5-year Fermi-LAT resolved fractions. The grey lines are the combined 95% CL AGN plus blazar predicted flux for the corresponding blazar contribution. The DGRB data (triangles) are from FS10 and the COMPTEL data (diamonds) are from Ref. [50].

in order to determine how well this class of models fits the DGRB and blazar population. For those models that fit the spectrum, we can determine the predicted values for the DGRB flux at the Fermi-LAT's 5-year sensitivities and determine the theoretical uncertainty on these predictions.

In another analysis of the contribution of blazars to the DGRB, the Fermi-LAT collaboration used the currently measured differential number distributions of blazars (dN/dF) and blazar gamma-ray index (Γ) distributions to estimate the contribution of unresolved blazars to the DGRB [4]. In that analysis, it was found that less than 20 percent of the DGRB can be accounted for by blazar emission. However, in that calculation, the assumption was made that the distribution of indices Γ is independent of sensitivity. Because less-luminous BL Lacs have significantly different indices than more luminous FSRQs, the overall distribution of indices should change as better sensitivity allows a greater fraction of BL Lacs to be detected.

Additionally, it was shown in Refs. [28, 39] that a basic power-law model does not fit the individual blazar spectra well, especially for the low-luminosity BL Lacs. A GLF plus SED model should overcome these issues. The GLF accounts for differing redshifts of blazars, so the relationship between flux sensitivity and luminosity detectability is well-defined. The SED accounts for the distribution of luminosities with energy, so a calculation around the IC peaks for BL Lacs should more realistically reproduce the contribution to the DGRB from blazars than a simple distribution of photon indices. This is especially important to incorporate when determining the contribution of unresolved low luminosity blazars to the DGRB, since they have much harder spectra than high luminosity blazars.

IV. 5-YEAR PREDICTIONS FOR BLAZARS AND THE DGRB

We adopt the 5-year predictions for a sensitivity to point-sources by Fermi-LAT of $S_5 = 2 \times 10^{-9}$ photons cm^{-2} s^{-1} above 100 MeV. This value is consistent with the Fermi-LAT collaboration's estimate of the LAT sensitivity to point sources with gamma-ray

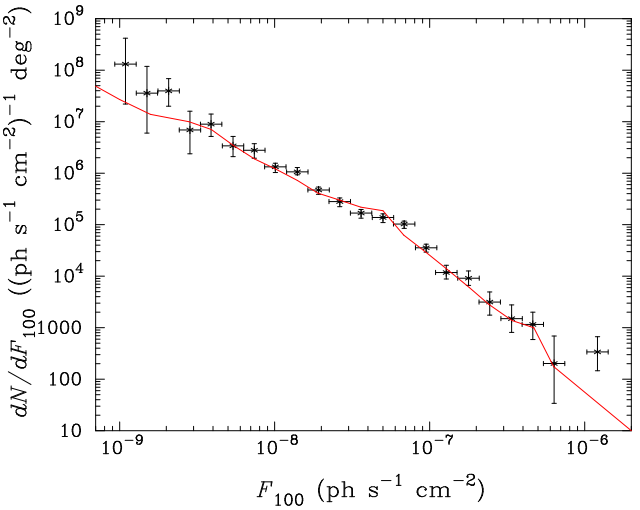

FIG. 4. Shown is the best-fit model for the source count distribution function dN/dF (solid line). The data are from Ref. [4]

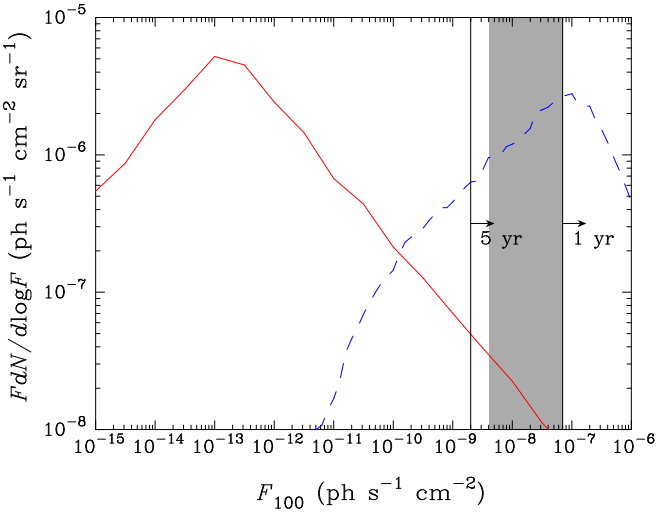

FIG. 5. Shown is the flux per logarithmic sensitivity for our best fit model. The dashed line is the flux coming from blazars and the solid line is the flux coming from non-blazar AGN. The vertical solid lines with arrows mark the sensitivity to *all* spectral-index sources at the Fermi-LAT 1-year and the projected 5-year sensitivity of Fermi-LAT. The gray boxed region indicates the range of sensitivity at 1-year to sources with the spectral indices of the bulk of the blazar population, as in Fig. 1.

index of ∼2 [54].[2] As discussed earlier, the majority of low-flux blazars are expected to be BL-Lacs, which predominantly have radio luminosity less than 10^{43} erg/s

[2] http://fermi.gsfc.nasa.gov/science/433-SRD-0001_CH-04.pdf

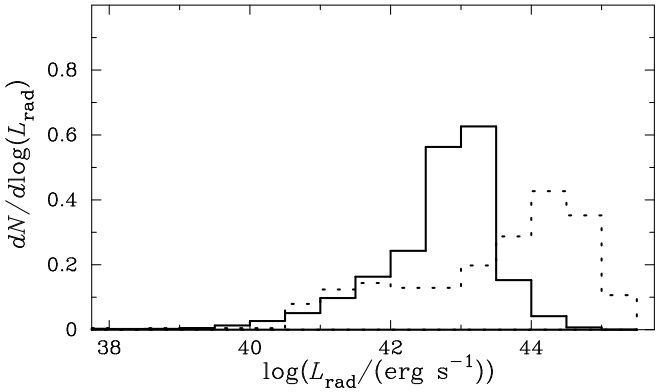

FIG. 6. Shown is the radio luminosity distribution of blazars. The solid line is our prediction for the distribution after 5 years of Fermi-LAT running. The dotted line is the current Fermi-LAT distribution for blazars [38]. Each distribution is independently normalized to unity.

[38]. Such low-luminosity blazars have gamma-ray indices of ∼2 or less, according to the blazar SED. Therefore, we find the use of $S_5 = 2{\times}10^{-9}$ photons cm^{-2} s^{-1} as the Fermi-LAT 5-year sensitivity to blazars of all gamma-ray indices to be a reasonable estimate.

To determine the total number of blazars detectable by the Fermi-LAT, we need to take Eq. (3.3) down to a sensitivity of S_5. Similarly, we can determine the total number of blazars in the sky by letting the sensitivity go to zero flux. With 95% CL, we predict that there are $5.4^{+1.8}_{-1.7} \times 10^4$ total blazars in the observable universe. Of these, 2415^{+240}_{-420} should be detectable by the Fermi-LAT after 5 years of running. The amount of flux coming from blazars per logarithmic sensitivity is shown in Fig. 5. Our prediction is that $94.7^{+1.9}_{-2.1}$% of blazar flux is expected to be resolved by the Fermi-LAT after 5 years, mostly at lower energies. In contrast, the flux for non-blazar AGN should not be appreciably resolved for another four orders of magnitude in sensitivity.

In addition to the number counts of blazars, we can also predict the distributions of blazars in luminosity and redshift. To get these distributions, we differentiate Eq. (3.3). The distribution of blazars in radio luminosity, shown in Fig. 6, shifts toward lower luminosities at better sensitivities. This is due to the FSRQ population being mostly resolved, whereas the new resolved sources at better sensitivities are mostly low-luminosity BL Lacs. The redshift distribution of blazars, Fig. 7, should shift toward higher redshifts as sensitivity improves. Because the FSRQ sample is mostly complete, it would be expected that the redshift distribution of BL Lacs, and blazars in general, should be roughly similar to the current redshift distribution of FSRQs. Our prediction of the redshift distribution of blazars after 5 years of Fermi-LAT running matches well with the current FSRQ distribution, which provides a verification of our theory and fit parameters. Note that the FSRQ sample is not to-

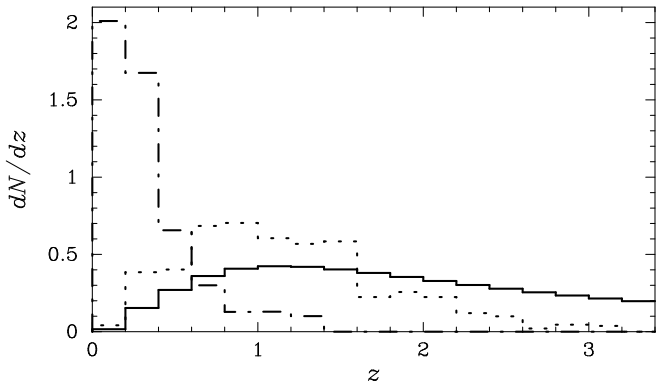

FIG. 7. Shown are the distribution in redshift of blazars. The solid line is our prediction for the distribution after 5 years of LAT running. The dotted line is the current Fermi-LAT measured distribution for FSRQs and the dot-dashed line is the current Fermi-LAT measured distribution for BL Lacs [38]. Each distributions is independently normalized to unity.

tally complete, and the objects to be resolved at at $z \gtrsim 2$ would be FSRQs. As can be seen in Fig. 9 of Ref. [38], the distribution of FSRQs reaches the current flux limit, so there remains a population of high-luminosity, soft spectral index, high redsift FSRQs to be resolved.

In our model, we fit the total blazar plus AGN flux to the DGRB spectrum for the spectrally-dependent sensitivity as described above. The model fit worked exceptionally well, indicating that a combination of blazar flux with the flux of non-blazar AGN makes up all the DGRB over a wide range in energies. With this fit, we then calculated what the combined flux should be after 5 years of Fermi-LAT observations, giving the sensitivity of 2×10^{-9} photons cm^{-2} s^{-1}. The upper and lower bounds of the 95% CL region of this calculation are given by the upper and lower forecast points in Fig. 3. We have included a 10% uncertainty on the non-blazar AGN flux in this error estimate to account for the error in the lowest energy bins' constraint on the AGN model. At 100 GeV, we expect the DGRB to decrease by a factor of 1.6 to 2.6 at the 95% CL upper and lower flux limits, whereas at 100 MeV the DGRB only decreases by a factor of 1.3 to 1.9. The difference in DGRB improvement is due to a greater fraction of the DGRB being due to blazars at high energies, while the non-blazar AGN flux dominates at low energies. Importantly, the resolution of sources can do better than the square root of exposure time due to the increased prevalence of easily-detected hard sources beyond, but near, the current point-source flux limit sensitivity.

V. CONCLUSIONS

We have shown that the DGRB can be composed entirely by gamma-rays produced in blazars and non-blazar AGNs. The LDDE plus SED-sequence is a physical model for the spectral evolution of a cosmologically-evolving blazar population contributing to the DGRB based on the unified AGN model for blazars. This model successfully accounts for the full DGRB spectrum as well as the flull blazar source count distribution function, which, unlike other approaches, are not used as components of the model. Independent of the non-blazar AGN component, the blazar model produces nearly the entire DGRB at the its highest measured energies. The small value of $\kappa \simeq 2.4 \times 10^{-6}$, the X-ray AGN fraction seen as blazars constrains this model to require a small fraction, $\lesssim$20% of X-ray AGN jets to be both properly oriented and sufficiently energetic in order to be gamma-ray emitters.

We found constraints on this model from the spectrum of the DGRB and source count distribution function dN/dF of blazars as observed by Fermi-LAT. Our results are consistent with previous work by Inoue & Totani [8] which employed EGRET spectral data to forecast the Fermi-LAT DGRB. We forecast that $94.7^{+1.9}_{-2.1}$% of the flux from blazars will be resolved into point sources by Fermi-LAT with 5 years of observation, with a corresponding reduction of the flux in the DGRB by a factor of $\sim$2 to 3 (95% CL) from the automatic removal of these sources in the measurement of the DGRB. This has significant consequences for the sensitivity of the DGRB measurement to dark matter annihilation, which we explore in a companion paper [55].

We predict that 2415^{+240}_{-420} blazars should be resolved, of $5.4^{+1.8}_{-1.7} \times 10^4$ total blazars in the universe (95% CL). Recent results of anisotropy in the DGRB also indicate the likely presence of an unresolved point source population [56]. Using tests with enhanced point source sensitivity, we find that future gamma-ray experiments at Fermi-LAT energies will resolve the blazar contribution to the DGRB such that the flux in the DGRB decreases as the square root of the point source sensitivity.

The LDDE plus SED-sequence model is more complex than the over-simplistic source-count method with a fixed spectral-index distribution adopted by the Fermi-LAT collaboration in FB10, yet it has *fewer* free parameters for the blazar population than the more simplified model (three versus four free for the blazar model, plus those fixed in the non-blazar AGN model in this work). Most importantly, the Fermi-LAT analysis of FB10 fixes the spectral index of the blazar population, and, crucially, does not include the hardening of the spectra of the unresolved low-luminosity blazar population. The hardening of spectra with lower luminisity has been seen by both EGRET [27] and Fermi-LAT (Fig. 1). The fixed spectrum forces the FB10 conclusion that only $\sim$16% of the GeV isotropic diffuse background could arise from blazars, and is also the case in other work using fixed

blazar spectra [30]. Other recent work with different blazar population models, including spectral shape variation [57], possible point source confusion [58], and BL Lac dominance of the unresolved portion [59] also find that a substantial portion of the DGRB could arise from the blazar population.

Overall, the SED sequence model of blazars and AGNs as the source of the DGRB is remarkably consistent with the measured DGRB spectrum and blazar source count distribution. The SED-sequence will continue to be improved with upcoming Fermi-LAT blazar data [60]. Further analyses of the type presented here, incorporating potential enhancements to the SED sequence model, the XLF of AGN, and general studies of observed blazar spectral properties, will further enlighten the understanding of the extragalactic gamma-ray sky.

ACKNOWLEDGMENTS

We would like to thank P. Agrawal, M. Ajello, J. Beacom, Z. Chacko, D. Malyshev and J. McEnery for useful discussions. KNA and JPH are supported by NSF Grant 07-57966 and NSF CAREER Award 09-55415. SB has been partially supported by MICNN, Spain, under contracts FPA 2007-60252 and Consolider-Ingenio CPAN CSD2007-00042 and by the Comunidad de Madrid through Proyecto HEPHACOS ESP-1473. SB acknowledges support from the CSIC grant JAE-DOC.

Appendix A: Blazar SED Sequence

The full SED fit is given as a function of radio luminosity ψ_R and the logarithm of rest-frame frequency x. We follow Ref. [8] in the formulation of the SED. The radio luminosity is used to distinguish between SEDs for blazars of different bolometric luminosity. This separation of SED by total luminosity should account for the difference in spectral index seen by the Fermi-LAT between higher-luminosity FSRQs and lower-luminosity BL Lacs [28, 39, 40].

$$x \equiv \log_{10}(\nu/\mathrm{Hz}), \tag{A1}$$

$$\psi(x;\psi_R) \equiv \log_{10}[\frac{\nu L_\nu(\nu(x), P(\psi_R))}{\mathrm{erg\ s^{-1}}}], \tag{A2}$$

$$\psi_R \equiv \psi(x = 9.698). \tag{A3}$$

The full model is the sum of a synchrotron $[\psi_s(x)]$ and inverse Compton $[\psi_c(x)]$ component.

$$\psi(x) = \log_{10}[10^{\psi_s(x)} + 10^{\psi_c(x)}]. \tag{A4}$$

Each component is parameterized as the sum of a lower-frequency linear part and a higher-frequency parabolic part. Here, $x_{tr,s}$ and $x_{tr,c}$ are the frequencies where the linear part transitions to the parabolic part for the synchrotron and IC component. The linear parts are written as:

$$\psi_{s1}(x) \equiv (1-\alpha_s)(x - x_R) + \psi_R \ (x < x_{tr,s}), \tag{A5}$$

$$\psi_{c1}(x) \equiv (1-\alpha_c)(x - x_X) + \psi_X \ (x < x_{tr,c}), \tag{A6}$$

where $\alpha_s = 0.2$ and $\alpha_c = 0.6$ are the $L_\nu \propto \nu^\alpha$ indices in the radio and hard X-ray bands, respectively. The characteristic radio and hard X-ray frequencies are $x_R = 9.698$ and $x_X = 17.383$. The radio luminosity ψ_R is an input parameter to the theory and the hard X-ray luminosity is fitted to the data as:

$$\psi_X = \begin{cases} (\psi_R - 43) + 43.17 & \psi_R \le 43 \\ 1.40(\psi_R - 43) + 43.17 & 43 < \psi_R \le 46.68 \\ 1.40(46.68 - 43) + 43.17 & \psi_R > 46.68\ . \end{cases} \tag{A7}$$

The parameter ψ_X is kept constant for $\psi_R > 46.68$ because the continuity of the IC component cannot be satisfied above this value. However, this hard X-ray luminosity corresponds to a gamma-ray luminosity well above the maximum detected gamma-ray luminosity, so it does not affect the calculation of the DGRB.

The parabolic parts of the components are parameterized as:

$$\psi_{s2}(x) \equiv \psi_{s,p} - [(x - x_s)/\sigma]^2 \ (x \ge x_{tr,s}), \tag{A8}$$

$$\psi_{c2}(x) \equiv \psi_{c,p} - [(x - x_c)/\sigma]^2 \ (x \ge x_{tr,c}), \tag{A9}$$

where x_s and x_c are the synchrotron and IC peak frequencies, $\psi_{s,p}$ and $\psi_{c,p}$ are the synchrotron and IC peak luminosities, and σ is the width of the parabolas.

By requiring continuity of the synchrotron component from the linear to parabolic parts, we have:

$$\psi_{s,p} = (1-\alpha_s)(x_{tr,s} - x_R) + \psi_R + \left(\frac{x_{tr,s} - x_s}{\sigma}\right)^2\ . \tag{A10}$$

Similarly, the continuity of the IC component gives:

$$x_{tr,c} = \frac{-\zeta - \sqrt{\zeta^2 - 4\eta}}{2}, \tag{A11}$$

$$\zeta = \sigma^2(1-\alpha_c) - 2x_c, \tag{A12}$$

$$\eta = x_c^2 + \sigma^2[\psi_X - x_X(1-\alpha_c) - \psi_{c,p}]\ . \tag{A13}$$

By inspection:

$$x_{tr,s} = 10.699, \tag{A14}$$

$$x_c = x_s + 8.699\ . \tag{A15}$$

Fitting to data, the rest of the parameters are given by:

$$x_s = \begin{cases} -0.88(\psi_R - 43) + 14.47 & \psi_R \le 43 \\ -0.40(\psi_R - 43) + 14.47 & \psi_R > 43 \end{cases} \tag{A16}$$

$$\sigma = \begin{cases} 0.0891 x_s + 1.78 & \psi_R \le 43 \\ [2(x_s - x_{tr,s})/(1-\alpha_s)]^{1/2} & \psi_R > 43 \end{cases} \tag{A17}$$

$$\psi_{c,p} = \begin{cases} \psi_{s,p} & \psi_R \le 43 \\ 1.77(\psi_R - 43)^{0.718} + 45.3 & \psi_R > 43\ . \end{cases} \tag{A18}$$

These parameters have been chosen such that the luminosity changes continuously with ψ_R over all luminosities and to make the synchrotron linear-to-parabolic transition smooth for large ψ_R.

Appendix B: X-ray Luminosity Function

The X-ray luminosity function ρ_X is the comoving number density of AGN per unit X-ray AGN disk luminosity L_X. The model of Refs. [29, 41] give the distribution as:

$$\rho_X(L_X, z) = \rho_X(L_X, 0) f(L_X, z). \tag{B1}$$

The present distribution is given by

$$\rho_X(L_X, 0) = \frac{A_X}{L_X ln(10)} \left[\left(\frac{L_X}{L_X^*} \right)^{\gamma_1} + \left(\frac{L_X}{L_X^*} \right)^{\gamma_2} \right]^{-1}. \tag{B2}$$

The density evolution is given by

$$f(L_X, z) = \begin{cases} (1+z)^{p_1} & z \leq z_c(L_X) \\ (1+z_c(L_X))^{p_1} \left(\frac{1+z}{1+z_c(L_X)} \right)^{p_2} & z > z_c(L_X). \end{cases} \tag{B3}$$

The peak evolution happens at z_c, given by

$$z_c(L_X) = \begin{cases} z_c^* & L_X \geq L_a \\ z_c^* (L_X/L_a)^{\alpha} & L_X < L_a. \end{cases} \tag{B4}$$

The evolution indices p_1 and p_2 are

$$p_1 = p_1^* + \beta_1 [\log_{10}(L_X) - 44.0] \tag{B5}$$

$$p_2 = p_2^* + \beta_2 [\log_{10}(L_X) - 44.0]. \tag{B6}$$

If $\gamma_1 > 1$, then the integrated background flux diverges, so we set the minimum gamma-ray luminosity to $L_{\gamma,\rm min} = 10^{42}$ erg/s. This is an order of magnitude lower than any Fermi-LAT observed blazar, and the results are not sensitive to this value being lowered slightly [28, 39].

Table 1

Parameters for the AGN XLF		
Parameter	Ueda et al. 2003	Hasinger et al. 2005
A_X (Mpc^{-3})	5.04×10^{-6}	2.62×10^{-7}
$log_{10} L_X^*$	$43.94^{+0.21}_{-0.26}$	43.94 ± 0.11
γ_2	2.23 ± 0.13	2.57 ± 0.16
z_c^*	1.9, fixed	1.96 ± 0.15
$log_{10} L_a$	44.6, fixed	44.67, fixed
α	0.335 ± 0.07	0.21 ± 0.04
p_1^*	4.23 ± 0.39	4.7 ± 0.3
p_2^*	-1.5, fixed	-1.5 ± 0.7
β_1	0.0, fixed	0.7 ± 0.3
β_2	0.0, fixed	0.6 ± 0.8
Note: Luminosities are in erg/s		

[1] C. E. Fichtel *et al.*, Astrophys. J. **198**, 163 (1975); Astrophys. J. Lett. **217**, L9 (1977); C. E. Fichtel, G. A. Simpson, and D. J. Thompson, Astrophys. J. **222**, 833 (1978); D. J. Thompson and C. E. Fichtel, Astron. & Astrophys. **109**, 352 (1982).

[2] P. Sreekumar *et al.*, Astrophys. J. **494**, 523 (1998), arXiv:astro-ph/9709257.

[3] A. A. Abdo *et al.* (Fermi-LAT Collaboration), Phys. Rev. Lett. **104**, 101101 (2010), arXiv:1002.3603 [astro-ph.HE].

[4] A. A. Abdo *et al.* (Fermi-LAT Collaboration), Astrophys. J. **720**, 435 (2010), arXiv:1003.0895 [astro-ph.CO].

[5] A. A. Abdo *et al.* (Fermi-LAT Collaboration), JCAP **1004**, 014 (2010), arXiv:1002.4415 [astro-ph.CO].

[6] K. N. Abazajian, P. Agrawal, Z. Chacko, and C. Kilic, JCAP **1011**, 041 (2010), arXiv:1002.3820 [astro-ph.HE].

[7] E. A. Baltz *et al.*, JCAP **0807**, 013 (2008), arXiv:0806.2911 [astro-ph].

[8] Y. Inoue and T. Totani, Astrophys. J. **702**, 523 (2009), arXiv:0810.3580 [astro-ph].

[9] Y. Inoue *et al.*, (2010), arXiv:1001.0103 [astro-ph.HE].

[10] Y. Inoue, T. Totani, and Y. Ueda, Astrophys. J. Lett. **672**, L5 (2008), arXiv:0709.3877.

[11] B. D. Fields, V. Pavlidou, and T. Prodanovic, Astrophys.J. **722**, L199 (2010), arXiv:1003.3647 [astro-ph.CO].

[12] C. A. Faucher-Giguere and A. Loeb, JCAP **1001**, 005 (2010), arXiv:0904.3102 [astro-ph.HE].

[13] J. M. Siegal-Gaskins, R. Reesman, V. Pavlidou, S. Profumo, and T. P. Walker, (2010), arXiv:1011.5501 [astro-ph.HE].

[14] S. Ando and E. Komatsu, Phys. Rev. **D73**, 023521 (2006), arXiv:astro-ph/0512217; S. Ando, E. Komatsu, T. Narumoto, and T. Totani, **D75**, 063519 (2007), arXiv:astro-ph/0612467; F. Miniati, S. M. Koushiappas, and T. Di Matteo, Astrophys. J. **667**, L1 (2007), arXiv:astro-ph/0702083; J. M. Siegal-Gaskins, JCAP **0810**, 040 (2008), arXiv:0807.1328 [astro-ph]; J. M. Siegal-Gaskins and V. Pavlidou, Phys. Rev. Lett. **102**, 241301 (2009), arXiv:0901.3776 [astro-ph.HE]; B. S. Hensley, J. M. Siegal-Gaskins, and V. Pavlidou, Astrophys. J. **723**, 277 (2010), arXiv:0912.1854 [astro-ph.CO]; M. Fornasa, L. Pieri, G. Bertone, and E. Branchini, Phys. Rev. **D80**, 023518 (2009), arXiv:0901.2921 [astro-ph].

[15] F. W. Stecker and M. H. Salamon, Astrophys. J. **464**, 600 (1996), arXiv:astro-ph/9601120.

[16] F. W. Stecker, M. H. Salamon, and M. A. Malkan, Astrophys. J. Lett. **410**, L71 (1993).

[17] P. Padovani *et al.*, Mon. Not. Roy. Astron. Soc. **260**, L21 (1993).

[18] M. H. Salamon and F. W. Stecker, Astrophys. J. Lett. **430**, L21 (1994).

[19] J. Chiang *et al.*, Astrophys. J. **452**, 156 (1995).

[20] J. Chiang and R. Mukherjee, Astrophys. J. **496**, 752 (1998).

[21] A. Mücke and M. Pohl, Mon. Not. Roy. Astron. Soc. **312**, 177 (2000).

[22] P. Giommi *et al.*, Astron. Astrophys. **445**, 843 (2006), arXiv:astro-ph/0508034.

[23] T. Narumoto and T. Totani, Astrophys. J. **643**, 81 (2006), arXiv:astro-ph/0602178.

[24] C. D. Dermer, Astrophys. J. **659**, 958 (2007), arXiv:astro-ph/0605402.

[25] V. Pavlidou and T. M. Venters, Astrophys. J. **673**, 114 (2008), arXiv:0710.0002.

[26] D. Bhattacharya, P. Sreekumar, and R. Mukherjee, Res. Astron. Astrophys. **9**, 85 (2009), arXiv:0811.4388 [astro-ph].

[27] G. Fossati *et al.*, Mon. Not. Roy. Astron. Soc. **289**, 136 (1997), arXiv:astro-ph/9704113; **299**, 433 (1998), arXiv:astro-ph/9804103; D. Donato *et al.*, Astron. & Astrophys. **375**, 739 (2001), arXiv:astro-ph/0105203.

[28] A. A. Abdo *et al.* (Fermi-LAT Collaboration), Astrophys. J. **710**, 1271 (2010).

[29] Y. Ueda, M. Akiyama, K. Ohta, and T. Miyaji, Astrophys. J. **598**, 886 (2003), arXiv:astro-ph/0308140.

[30] D. Malyshev and D. W. Hogg, (2011), arXiv:1104.0010 [astro-ph.CO].

[31] R. C. Hartman *et al.*, Astrophys. J. Supp. **123**, 79 (1999).

[32] C. M. Urry and P. Padovani, Pub. Astron. Soc. Pacific **107**, 803 (1995), arXiv:astro-ph/9506063.

[33] R. D. Blandford and A. Konigl, Astrophys. J. **232**, 34 (1979).

[34] C. D. Dermer and N. Gehrels, Astrophys. J. **447**, 103 (1995).

[35] E. Komatsu *et al.* (WMAP Collaboration), Astrophys.J.Suppl. **192**, 18 (2011), arXiv:1001.4538 [astro-ph.CO].

[36] A. W. Strong and I. V. Moskalenko, Astrophys. J. **509**, 212 (1998), arXiv:astro-ph/9807150.

[37] A. W. Strong, I. V. Moskalenko, and O. Reimer, Astrophys. J. **537**, 763 (2000), arXiv:astro-ph/9811296.

[38] A. A. Abdo *et al.* (Fermi-LAT Collaboration), Astrophys. J. **715**, 429 (2010), arXiv:1002.0150 [astro-ph.HE].

[39] A. A. Abdo *et al.* (Fermi-LAT Collaboration), Astrophys. J. **716**, 30 (2010), arXiv:0912.2040 [astro-ph.CO].

[40] G. Ghisellini, L. Maraschi, and F. Tavecchio, Mon. Not. Roy. Astron. Soc. **396**, L105 (2009), arXiv:0903.2043 [astro-ph.CO].

[41] G. Hasinger, T. Miyaji, and M. Schmidt, Astron. Astrophys. **441**, 417 (2005), arXiv:astro-ph/0506118.

[42] H. Falcke, E. Koerding, and S. Markoff, Astron. Astrophys. **414**, 895 (2004), arXiv:astro-ph/0305335.

[43] A. Merloni, S. Heinz, and T. Di Matteo, Mon. Not. Roy. Astron. Soc. **345**, 1057 (2003), arXiv:astro-ph/0305261.

[44] E. Gallo *et al.*, Nature **436**, 819 (2005), arXiv:astro-ph/0508228.

[45] A. Marconi *et al.*, Mon. Not. Roy. Astron. Soc. **351**, 169 (2004), arXiv:astro-ph/0311619.

[46] R. C. Gilmore *et al.*, Mon. Not. Roy. Astron. Soc. **399**, 1694 (2009), arXiv:0905.1144 [astro-ph.CO].

[47] A. A. Abdo *et al.* (Fermi-LAT Collaboration), Astrophys. J. **723**, 1082 (2010), arXiv:1005.0996 [astro-ph.HE].

[48] S. C. Kappadath *et al.*, Astron. & Astrophys. Supp. **120**, C619+ (1996).

[49] Y. Ueda, M. Akiyama, K. Ohta, and T. Miyaji, Astrophys.J. **598**, 886 (2003), arXiv:astro-ph/0308140 [astro-ph].

[50] K. Watanabe, D. H. Hartmann, M. D. Leising, and L. S. The, Nucl. Phys. **A718**, 425 (2003), arXiv:astro-ph/0306161.

[51] A. Pushkarev, Y. Kovalev, M. Lister, and T. Savolainen, (2009), arXiv:0910.1813 [astro-ph.CO].

[52] J. H. Krolik, *Active galactic nuclei : from the central black hole to the galactic environment* (Princeton University Press, Princeton, N.J., 1999).

[53] Y. Inoue, S. Inoue, M. A. R. Kobayashi, T. Totani, J. Kataoka, and R. Sato, Mon. Not. Roy. Astron. Soc. **411**, 464 (2011), arXiv:1007.4379 [astro-ph.HE].

[54] W. B. Atwood *et al.* (LAT), Astrophys. J. **697**, 1071 (2009), arXiv:0902.1089 [astro-ph.IM].

[55] K. N. Abazajian, S. Blanchet, and J. P. Harding, (2010), arXiv:1011.5090 [hep-ph].

[56] G. Gomez-Vargas *et al.* (Fermi-LAT Collaboration), (2010), arXiv:1012.0755 [astro-ph.HE].

[57] T. M. Venters and V. Pavlidou, Astrophys. J., in press (2011), arXiv:1105.0372 [astro-ph.HE].

[58] F. W. Stecker and T. M. Venters, (2010), arXiv:1012.3678 [astro-ph.HE].

[59] A. Neronov and D. Semikoz, (2011), arXiv:1103.3484 [astro-ph.CO].

[60] E. T. Meyer, G. Fossati, M. Georganopoulos, and M. L. Lister, (2011), arXiv:1107.5105 [astro-ph.CO].